SUPPLEMENTARY INFORMATION

Convergence of Biological Nitration and Nitrosation via Symmetrical Nitrous Anhydride

Dario A. Vitturi[1], Lucia Minarrieta[2], Sonia R. Salvatore[1], Edward M. Postlethwait[3], Marco Fazzari[1,4], Gerardo Ferrer-Sueta[5,6], Jack R. Lancaster Jr.[1,7,8], Bruce A. Freeman[1,#] and Francisco J. Schopfer[1,#] .

Departments of [1]Pharmacology and Chemical Biology, [7]Medicine and [8]Surgery. University of Pittsburgh. Pittsburgh, PA, USA. [2]Cátedra de Inmunología, [5] Laboratorio de Fisicoquímica Biológica, and [6]Center for Free Radical and Biomedical Research. Universidad de la República, Montevideo, Uruguay. [3]Department of Environmental Health Sciences, University of Alabama at Birmingham, Birmingham, AL, USA. [4]Fondazione Ri.MED, Palermo, Italy.

[#]To whom correspondence may be addressed: Bruce A. Freeman, Ph.D. or Francisco J. Schopfer, Ph.D., Department of Pharmacology & Chemical Biology, Thomas E. Starzl Biomedical Science Tower E1340, 200 Lothrop St, University of Pittsburgh, Pittsburgh, PA 15213, USA; Tel: 648-9319; Fax: (412) 648-2229; Email: freerad@pitt.edu or fjs2@pitt.edu.

SUPPLEMENTARY RESULTS

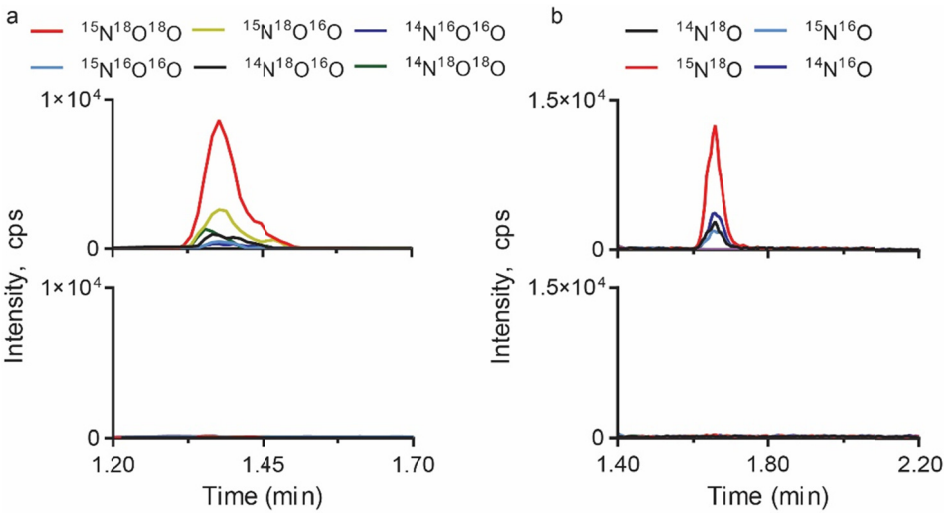

Supplementary Figure 1. NO_2^- does not mediate CLA nitration and GSH nitrosation in the absence of $^{\bullet}$NO. a, CLA (20 μM) and $^{15}N^{18}O_2^-$ (2 mM) were incubated for 100 min in 20 mM BisTris + 100 μM DTPA pH 7.0 and 25 ^{o}C in the presence (top panel) or absence (bottom panel) of 25 μM MNO. Representative LC-MS/MS traces show no formation of NO_2-CLA isotopologues in the absence of $^{\bullet}$NO donor. **b**, GSH (20 μM) and $^{15}N^{18}O_2^-$ (2 mM) were incubated for 120 min in 20 mM BisTris + 100 μM DTPA pH 7.0 and 25 ^{o}C in the presence (top panel) or absence (bottom panel) of 2.5 μM MNO. Representative traces demonstrate that GSNO formation was not detected in the absence of $^{\bullet}$NO donor.

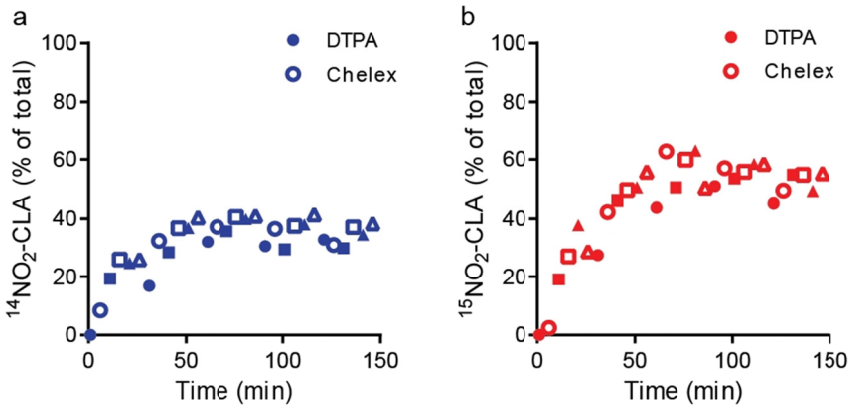

Supplementary Figure 2. NO_2^- dependent CLA nitration is independent of metal catalysis. Identical yields and distribution of $^{14}NO_2$-CLA (**a**) and $^{15}NO_2$-CLA (**b**) formation from CLA (20 μM) nitration in the presence of 200 μM $^{15}NO_2^-$ using either DTPA (100 μM) or Chelex treatment to remove adventitious metals from the reaction buffer (20 mM BisTris pH 7.0).

Nature Chemical Biology: doi:10.1038/nchembio.1814

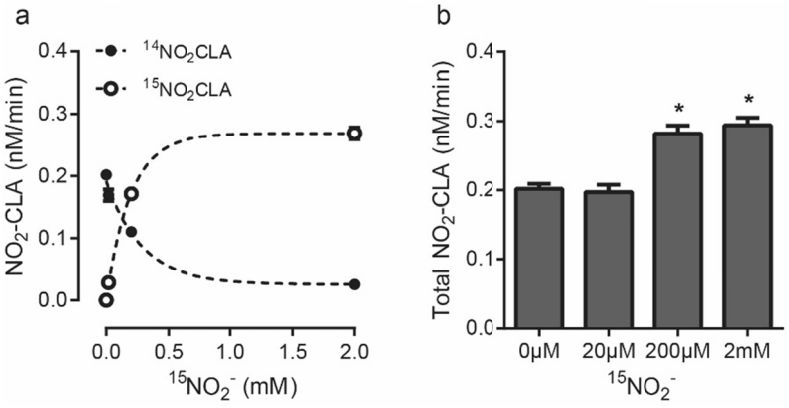

Supplementary Figure 3. $^{15}NO_2^-$ participates in CLA nitration in the absence of cellular components. a, Plot of initial rates of NO_2-CLA formation showing reciprocal modulation of the ^{14}N and ^{15}N containing products by $^{15}NO_2^-$. Data are means ±SE (n=4), with non-linear fits provided for illustrative purposes. **b**, The global initial rate of NO_2-CLA formation ($^{14}NO_2$-CLA + $^{15}NO_2$-CLA) is moderately increased by $^{15}NO_2^-$ concentration versus no-nitrite controls as determined by one way ANOVA and Bonferroni's multiple comparison test. Data are means ±SD (n=4), * $p < 0.0001$.

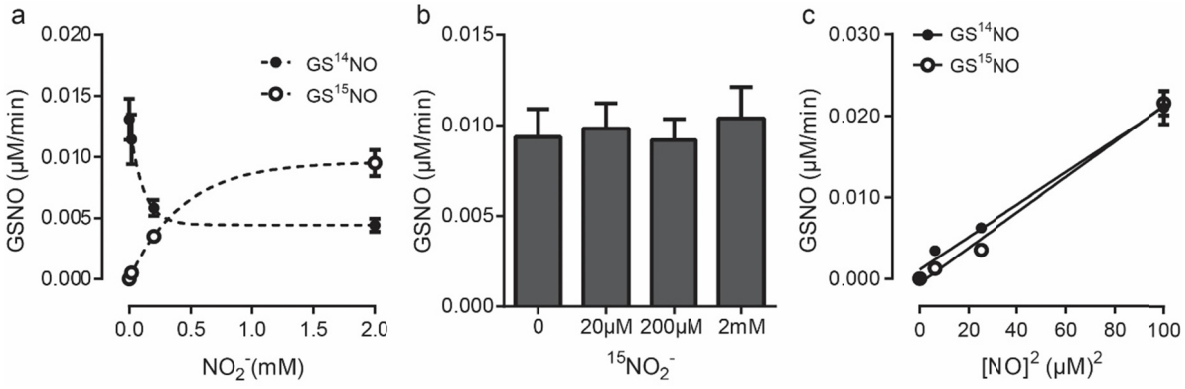

Supplementary Figure 4. $^{15}NO_2^-$ is incorporated into S-nitrosoglutathione in the presence of $^{\bullet}$NO. a, Initial $GS^{14}NO$ and $GS^{15}NO$ formation rates plotted versus $^{15}NO_2^-$ concentration illustrating reciprocal modulation of ^{14}N- and ^{15}N-containing products. Data are means ±SD (n=4), fits are provided for illustrative purposes. **b**, No effect of $^{15}NO_2^-$ in the global initial rate of GSNO formation as determined by one way ANOVA. Data are means ±SD (n=4). **c,** Initial rates of $GS^{14}NO$ and $GS^{15}NO$ formation are linearly dependent on $[^{\bullet}NO]^2$ (R2 > 0.99), consistent with a process limited by $^{\bullet}$NO autoxidation (20 μM GSH, 200 μM $^{15}NO_2^-$). Data are means ± SD (n=4).

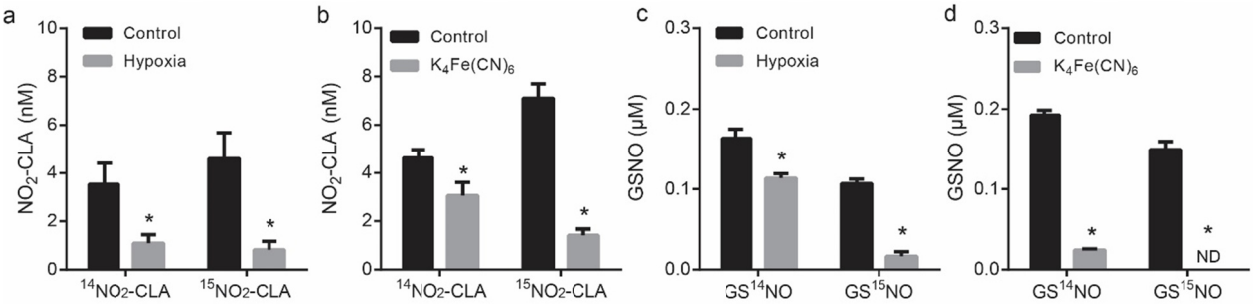

Supplementary Figure 5. $^{\bullet}NO_2$ is required for nitrite-dependent $^{15}NO_2$-CLA and GS^{15}NO formation. a-b, Formation of $^{14}NO_2$-CLA and $^{15}NO_2$-CLA (25 μM MNO, 200 μM $^{15}NO_2^-$, 90 minutes) is inhibited both under hypoxic conditions (a) and by 1mM $K_4Fe(CN)_6$ (b), * $p < 0.001$ versus corresponding control. **c-d,** GS^{14}NO and GS^{15}NO formation (2.5 μM MNO, 200 μM $^{15}NO_2^-$, 90 minutes) is inhibited by low oxygen tension (c) and 1mM $K_4Fe(CN)_6$ (d), * $p < 0.0001$ versus corresponding control. Data are mean ± SD (n=4) of independent experiments. Two-way ANOVA and Bonferroni's multiple comparison were used to test statistical significance.

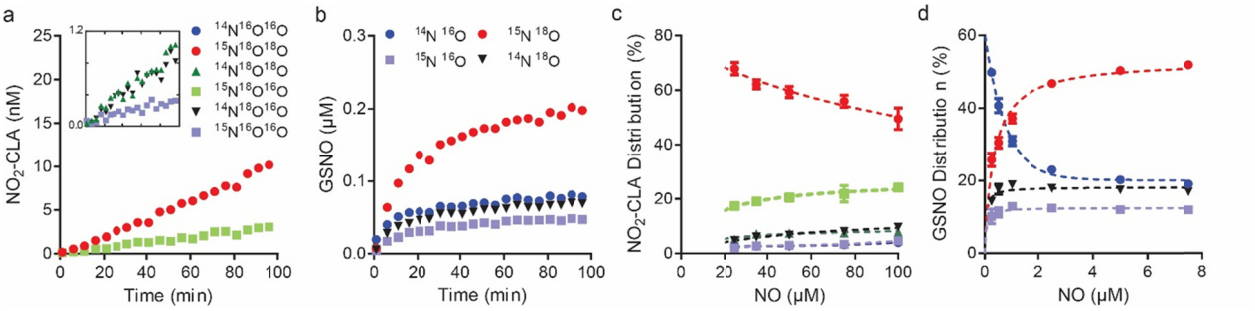

Supplementary Figure 6. NO_2^- incorporation into GSNO and NO_2-CLA is associated with symN_2O_3 formation. a, Time-dependent generation of mixed $^{14}N/^{15}N$ and $^{18}O/^{16}O$ NO_2-CLA isotopologues from the reaction of 2 mM $^{15}N^{18}O_2^-$ with of 25 μM MNO. Insert shows additional low-abundance NO_2-CLA isotopologues. Data are representative traces generated by combining time-staggered replicates (n=4). **b**, Formation of mixed $^{14}N/^{15}N$ and $^{18}O/^{16}O$ GSNO from 2.5 μM MNO and 2 mM $^{15}N^{18}O_2^-$. Traces represent four time-staggered replicates. **c**, NO_2-CLA distribution versus $^{\bullet}NO$ concentration in the presence of 2 mM $^{15}N^{18}O_2^-$. Data are mean ±SD (n=4), fits are provided for illustrative purposes. **d,** Percent GSNO distribution in the presence of 2 mM $^{15}N^{18}O_2^-$nitrite, with increased formation of isotopically-scrambled products at higher $^{\bullet}NO$ concentrations. Data are mean ±SD (n=4), fits are provided for illustrative purposes.

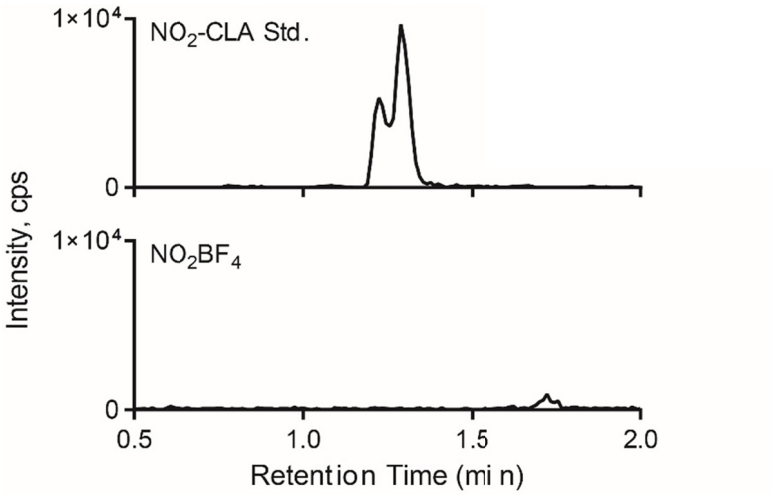

Supplementary Figure 7. NO_2^+ does not mediate NO_2-CLA CLA nitration. Representative LC-MS/MS traces showing no CLA (20 μM) nitration by NO_2BF_4 (50 μM) following 90 min incubation in 20 mM BisTris + 100 μM DTPA pH 7.0 and 25 ^{o}C (bottom panel). A NO_2-CLA standard is provided in the top panel for reference.

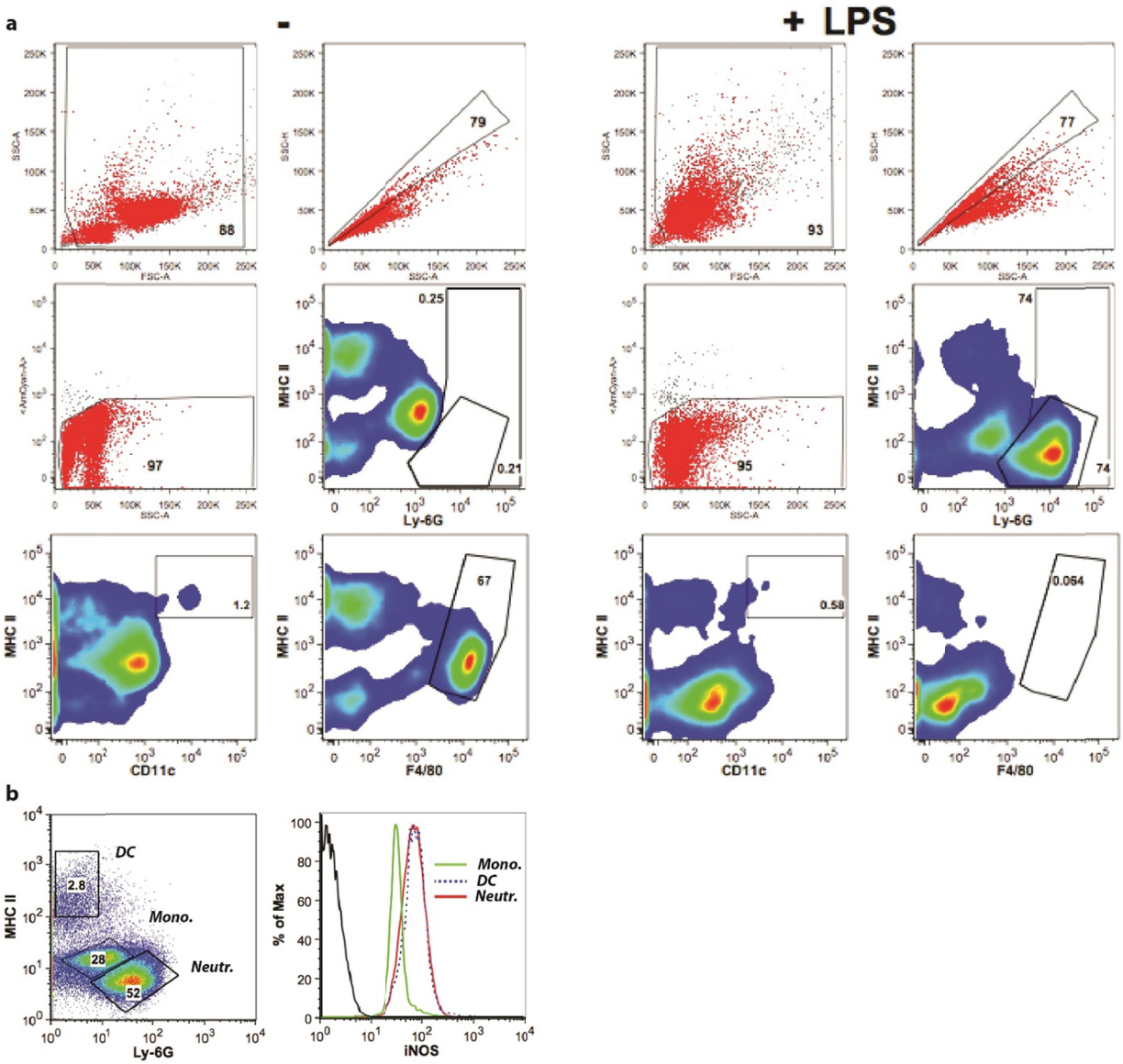

Supplementary Figure 8. Distribution of peritoneal cell subpopulations during LPS-induced inflammation. a, Intraperitoneal LPS injection in an incomplete Freund adjuvant emulsion leads to resident macrophage depletion (F480^{+}, MHCII^{INT}) and massive recruitment of neutrophils (Ly6G^{HI}, CD11b^{+}) and inflammatory monocytes (Ly6G^{INT},CD11b^{+}) 18 hours after treatment. Dendritic cells are also present (CD11c^{+}, MHCII^{HI}) in the peritoneal cavity. **b,** Distribution of iNOS expression among inflammatory cell subpopulations in LPS-treated mice.

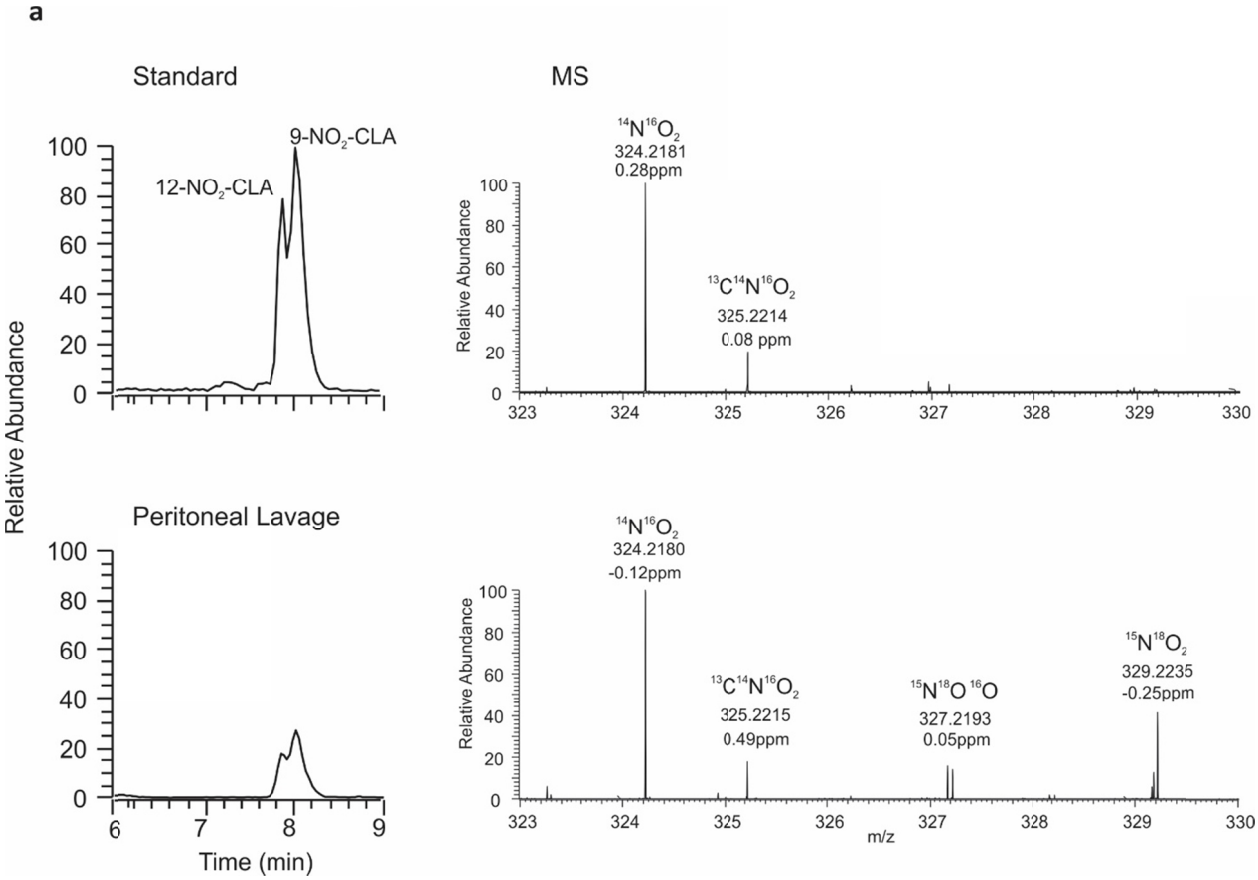
a
Standard
MS
9-NO2-CLA
12-NO2-CLA
Relative Abundance
14N16O2
324.2181
0.28ppm
13C14N16O2
325.2214
0.08 ppm
Peritoneal Lavage
14N16O2
324.2180
-0.12ppm
13C14N16O2
325.2215
0.49ppm
15N18O16O
327.2193
0.05ppm
15N18O2
329.2235
-0.25ppm
Time (min)
m/z

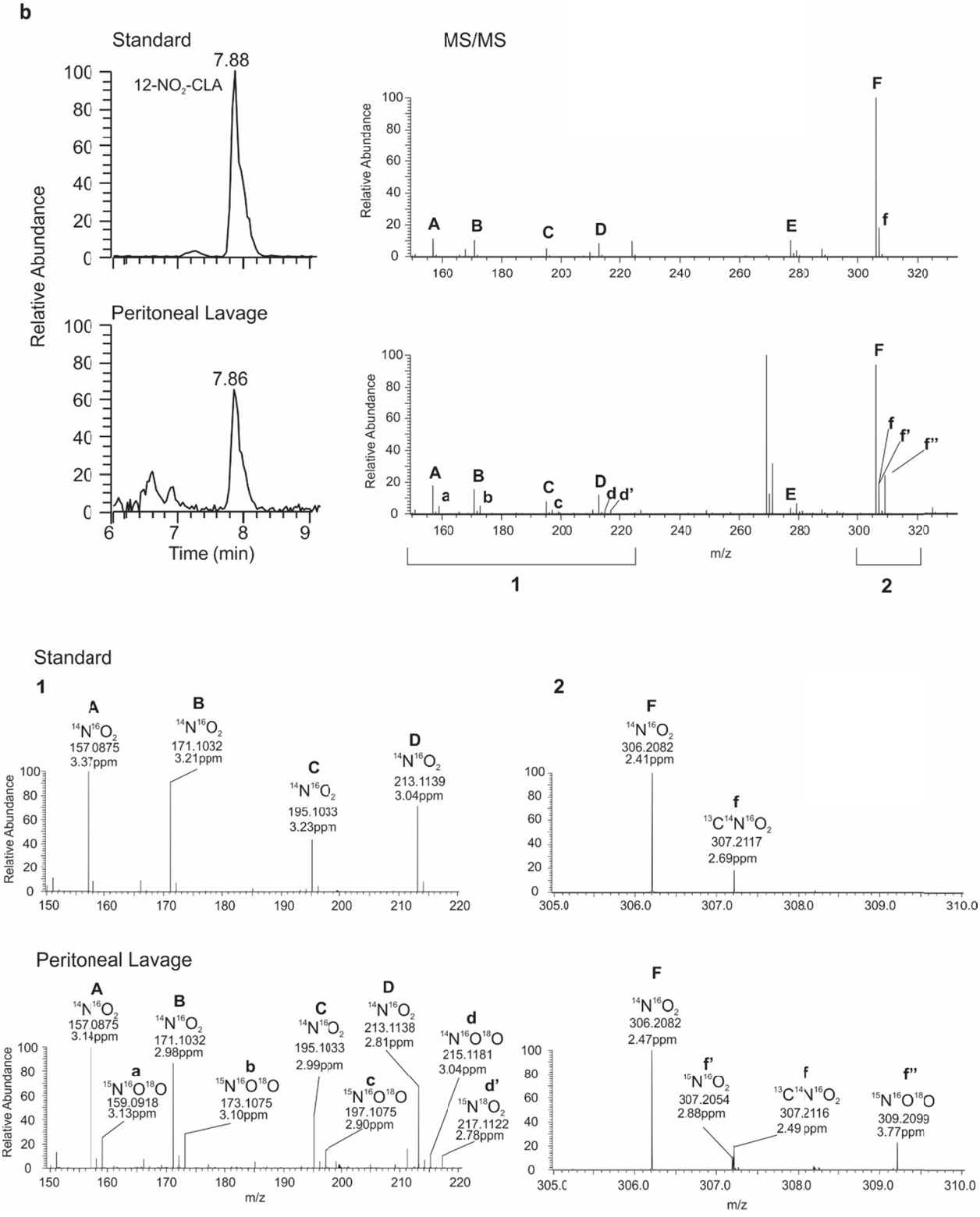
b
Standard
MS/MS
7.88
12-NO2-CLA
Relative Abundance
Peritoneal Lavage
7.86
Time (min)
m/z
1
2
Standard
1
2
Peritoneal Lavage
14N16O2 157.0875 3.37ppm
14N16O2 171.1032 3.21ppm
14N16O2 195.1033 3.23ppm
14N16O2 213.1139 3.04ppm
14N16O2 306.2082 2.41ppm
13C14N16O2 307.2117 2.69ppm
14N16O2 157.0875 3.14ppm
15N16O18O 159.0918 3.13ppm
14N16O2 171.1032 2.98ppm
15N16O18O 173.1075 3.10ppm
14N16O2 195.1033 2.99ppm
15N16O18O 197.1075 2.90ppm
14N16O2 213.1138 2.81ppm
14N16O18O 215.1181 3.04ppm
15N18O2 217.1122 2.78ppm
14N16O2 306.2082 2.47ppm
15N16O2 307.2054 2.88ppm
13C14N16O2 307.2116 2.49 ppm
15N16O18O 309.2099 3.77ppm

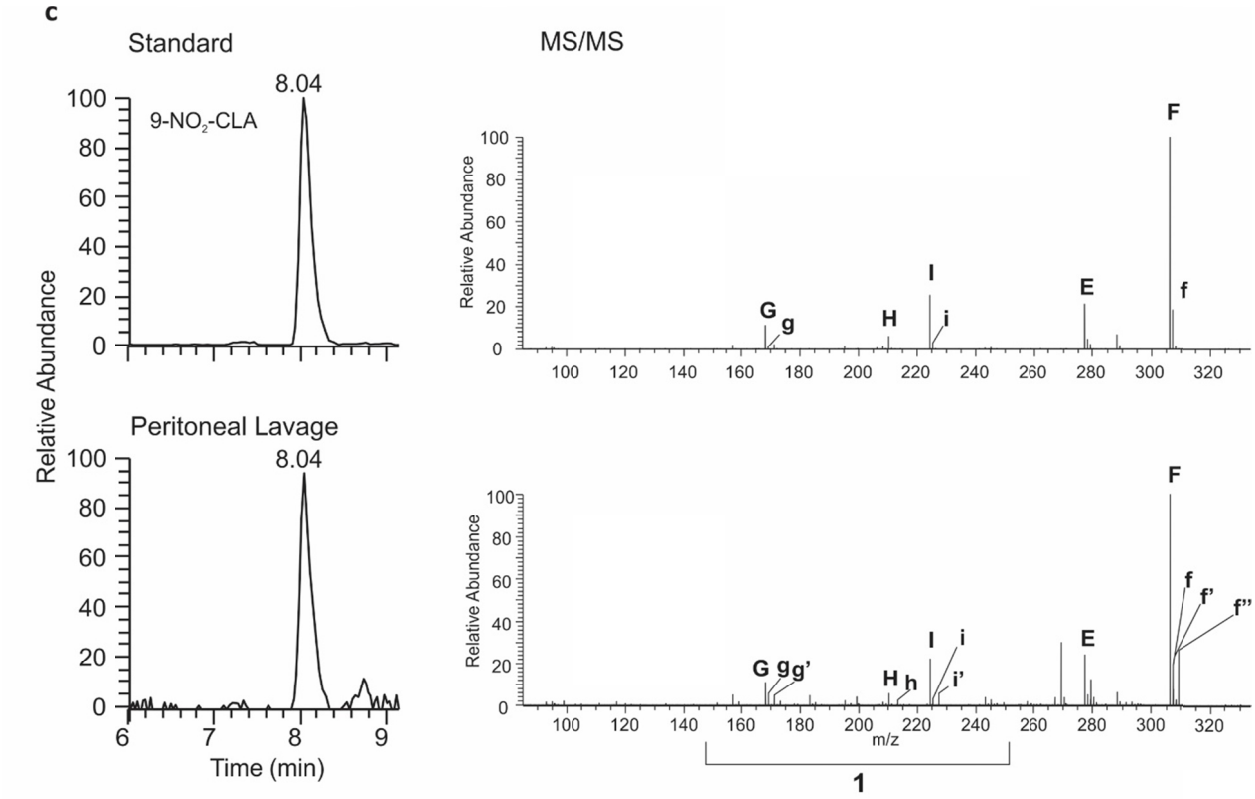
c
Standard
MS/MS
8.04
9-NO2-CLA
Relative Abundance
Peritoneal Lavage
8.04
Time (min)
F
I
E
f
G
g
H
i
f'
f''
g'
h
i'
m/z
1

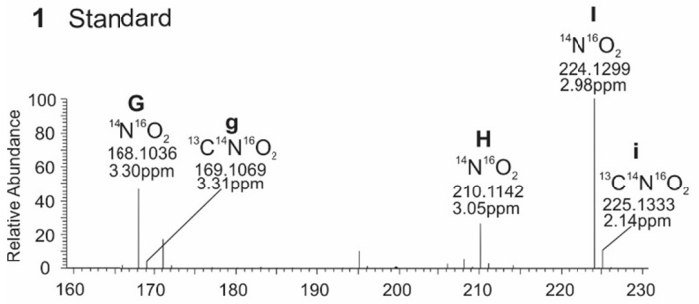
1 Standard
G
14N16O2
168.1036
3.30ppm
g
13C14N16O2
169.1069
3.31ppm
H
14N16O2
210.1142
3.05ppm
I
14N16O2
224.1299
2.98ppm
i
13C14N16O2
225.1333
2.14ppm
Relative Abundance

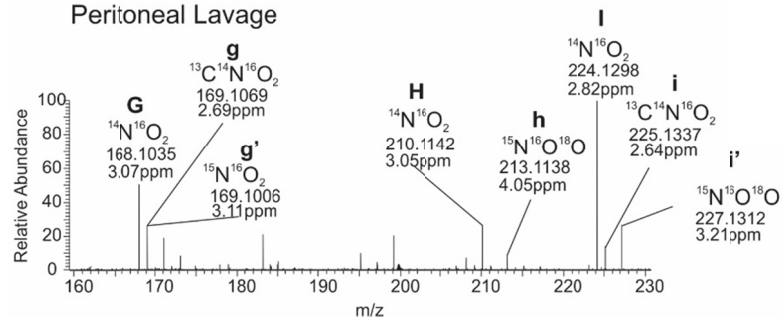
Peritoneal Lavage
G
14N16O2
168.1035
3.07ppm
g
13C14N16O2
169.1069
2.69ppm
g'
15N16O2
169.1006
3.11ppm
H
14N16O2
210.1142
3.05ppm
h
15N16O18O
213.1138
4.05ppm
I
14N16O2
224.1298
2.82ppm
i
13C14N16O2
225.1337
2.64ppm
i'
15N13O18O
227.1312
3.21ppm
Relative Abundance
m/z

Supplementary Figure 9. High resolution MS/MS analysis of $^{15}N^{18}O_2^-$-derived NO_2-CLA isotopologues generated during acute peritoneal inflammation. a, LC-MS/MS analysis revealed two positional isomers for each NO_2-CLA isotopologue, i.e. 9-NO_2-CLA and 12-NO_2-CLA. An identical chromatographic profile and retention times were observed for both synthetic standards (upper panel) and peritonitis plus $^{15}N^{18}O_2$ supplementation samples (lower panel). **b-c,** Individual high resolution MS/MS analysis of the positional 9-NO_2-CLA (**b**) and 12-NO_2-CLA (**c**) isomers and their corresponding containing isotopologues showed the expected losses of H_2O (Δ mass = 18.0106) and $H_2{}^{18}O$ (Δ mass = 20.0148) from the NO_2 group to form product ions with m/z 306.2082, 307.2054, and 309.2099 (peaks F, f' and f''). The naturally-occurring ^{13}C containing product ions were also resolved and were distinct from the ^{15}N products at a 60000 resolution (Panel b, peak f. Panel c, peaks g-i). Specific product ions derived from carbon chain fragmentation of the isotopologues further confirmed the incorporation of labeled NO_2^- and the formation of nitroalkene isomers identical to those observed in chemical reaction systems and *in vitro* cell culture models. In this regard, fragmentation of the isotopologues of 12-NO_2-CLA generated the same pattern of product ions as the synthetic standard and as previously reported (References 13 and 14 in the main text). In addition to the ^{13}C isotopes observed in both the synthetic 12-NO_2-CLA and the peritoneal inflammation sample, easily recognizable products ions containing isotopically-labeled O atoms were identified and confirmed at a 3 ppm resolution (Panel b, peaks A-D, a-d and d'). As previously reported, product ions stemming from carbon chain fragmentation of 12-NO_2-CLA lose their nitrogen as the result of a cyclization reaction, thus no ions containing ^{15}N are observed (Figure 5b). The same approach was used to characterize 9-NO_2-CLA isomers, where the fragmentation of this isomer is characterized by retaining the N atom. Biologically-generated 9-NO_2-CLA shows the same fragmentation pattern as synthetic 9-NO_2-CLA with the addition of the labeled ^{15}N and ^{18}O atoms confirmed at high resolution at the 3 ppm level (Panel c, peaks G-I, g'-i'). Corresponding structures and measured m/z for product ions detected in this figure are provided in Supplementary Table 2.

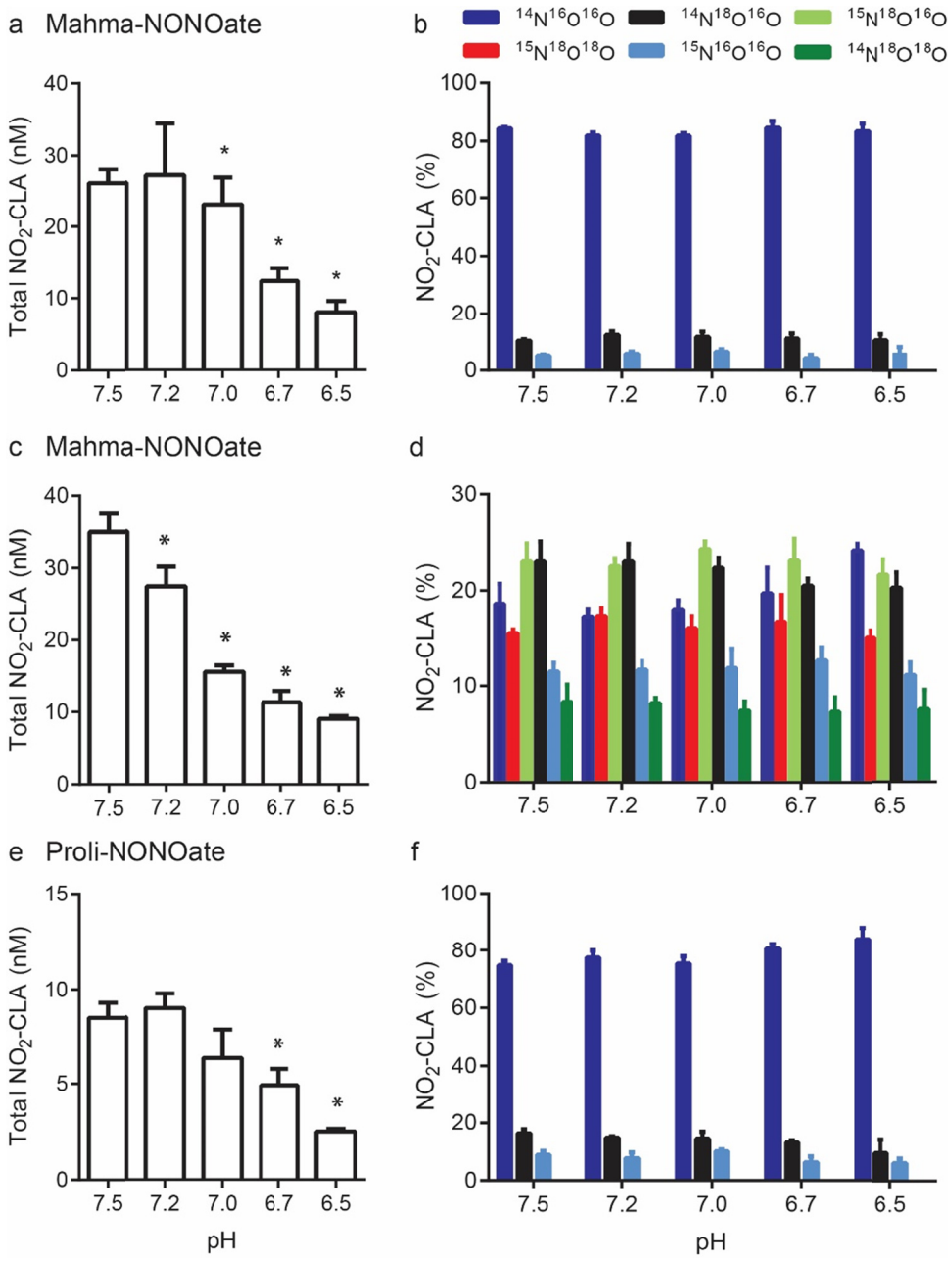

Supplementary Figure 10. pH dependence of CLA nitration by symN_2O_3. CLA nitration by 20 μM (**a-b**) and 200 μM (**c-d**) $^{15}N^{18}O_2^-$ was determined after 90 min incubations with 20 mM BisTris +100 μM DTPA and 25 μM mahma-NONOate at the indicated pH values. **e-f**, CLA nitration in the presence of 20 μM was induced by addition of 25 μM of the fast-releasing NO-donor proli-NONOate (half-life < 2 s) under the same conditions as before. For all panels, data are mean ± SD (n=4). Total CLA nitration was reduced at lower pH values as determined by one-way ANOVA analysis. * $p < 0.05$ versus pH = 7.5.

Supplementary Table 1. Exogenous and endogenous nitrite levels in peritoneal lavages 1 h post CLA/$^{15}N^{18}O_2^-$ injection.

Nitrite Injected	Peritoneal Nitrite (nmoles)					
	$[^{14}N]\ NO_2^-$		$[^{15}N]\ NO_2^-$		Total	% $[^{15}N]$
	Mean	SD	Mean	SD		
20 nmoles	3.61	± 0.71	0.18	± 0.15	3.78	4.7 %
200 nmoles	3.27	± 1.97	0.30	± 0.14	3.57	8.4 %

Supplementary Table 2. Structures, measured m/z, atomic composition and corresponding precursors for product ions generated from 9- and 12-NO_2-CLA isotopologues isolated from peritoneal lavages.

	Fragment Exp	Fragment Theoretical	Fragment Composition	Fragment Structure	NO_2-FA
A	157.0875	157.087	$C_8H_{13}O_3^-$	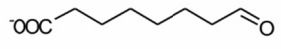	**12-NO_2-CLA** Exp Mass: 324.2180 Exact Mass: 324.2180 or **12-$^{15}N^{18}O^{16}O$-CLA** Exp Mass: 327.2193 Exact Mass:327.2193
B	171.1032	171.1027	$C_9H_{15}O_3^-$	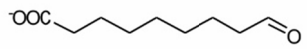	
C	195.1033	195.1027	$C_{11}H_{15}O_3^-$	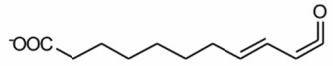	
D	213.1138	213.1132	$C_{11}H_{17}O_4^-$	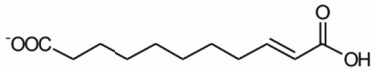	
G	168.1035	168.103	$C_9H_{14}NO_2^-$	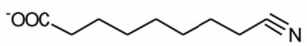	**9-NO_2-CLA** Exp Mass: 324.2180 Exact Mass: 324.2180
H	210.1142	210.1136	$C_{11}H_{16}NO_3^-$	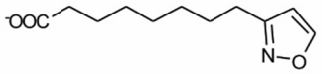	
I	224.1298	224.1292	$C_{12}H_{18}NO_3^-$	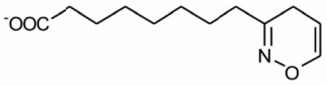	
a	159.0918	159.0913	$C_8H_{13}{}^{18}O^{16}O_2^-$	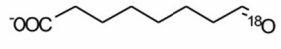	**12-$^{15}N^{18}O^{16}O$-CLA** Exp Mass: 327.2193 Exact Mass:327.2193 or **12-$^{15}N^{18}O_2$-CLA** Exp Mass: 329.2234 Exact Mass: 329.2236
b	173.1075	173.1069	$C_9H_{15}{}^{18}O^{16}O_2^-$	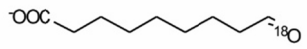	
c	197.1075	197.1069	$C_{11}H_{15}{}^{18}O^{16}O_2^-$	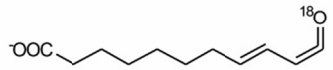	
d	215.1182	215.1175	$C_{11}H_{17}{}^{18}O^{16}O_3^-$	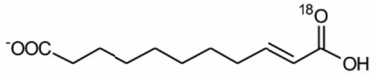	
d'	217.1122	217.1217	$C_{11}H_{17}{}^{18}O_2{}^{16}O_2^-$	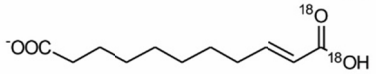	
g'	169.1006	169.100	$C_9H_{14}{}^{15}NO_2^-$	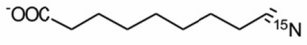	**9-$^{15}N^{18}O^{16}O$-CLA** Exp Mass: 327.2193 Exact Mass:327.2193 or **9-$^{15}N^{18}O_2$-CLA** Exp Mass: 329.2234 Exact Mass: 329.2236
h	213.1138	213.1148	$C_{11}H_{16}{}^{15}N^{18}O^{16}O_2^-$	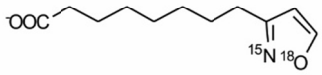	
i'	227.1312	227.1305	$C_{12}H_{18}{}^{15}N^{18}O^{16}O_2^-$